Reaction Kinetics, Mechanisms and Catalysis (2018) 125:983–994
https://doi.org/10.1007/s11144-018-1456-3

The effect of molybdenum on the characteristics and catalytic properties of M/$Cs_{1.5}H_{1.5}PW_{12}O_{40}$/$Al_2O_3$ (M = Ni or/and Mo) nanocatalysts in the hydrocracking of *n*-decane

Hoda Amirmoghadam[1] · Moayad Hossaini Sadr[1,2] · Hamidreza Aghabozorg[3] · Fathoallah Salehirad[3] · Akbar Irandoukht[3]

Received: 16 April 2018 / Accepted: 10 August 2018 / Published online: 21 August 2018

Abstract

In this research, M/$Cs_{1.5}H_{1.5}PW/Al_2O_3$ (M = Ni or/and Mo) nanocatalysts were prepared via 2 steps with the impregnation method and the effect of molybdenum on the characteristic and catalytic properties of the prepared samples was studied. The synthesized samples were characterized by X-ray diffraction (XRD), temperature programmed reduction, temperature programmed desorption (TPD), and energy dispersive X-ray spectroscopy techniques. Morphology of the samples was studied by field emission scanning electron microscope (FESEM) and surface area, pore volume and pore size of the compounds were measured by BET method. In the XRD patterns of the prepared catalysts, the $H_3PW_{12}O_{40}$ phase was observed. The FESEM images showed that the synthesized particles were in nanoscale. The results of TPD studies indicated that the total acid site of Ni–Mo/$Cs_{1.5}H_{1.5}PW/Al_2O_3$ catalyst was more than the others. The catalytic activity of the nanocatalysts in hydrocracking of *n*-decane indicated that Ni–Mo/$Cs_{1.5}H_{1.5}PW/Al_2O_3$ nanocatalyst had the highest catalytic activity.

Keywords Heteropoly acid · Molybdenum · Nanocatalyst · Hydrocracking · Nickel · Alumina

✉ Hamidreza Aghabozorg
aghabozorghr@ripi.ir

[1] Department of Chemistry, Science and Research Branch, Islamic Azad University, Tehran, Iran

[2] Department of Chemistry, Tarbiat Moallem University of Azarbaijan, Tabriz, Iran

[3] Research Institute of Petroleum Industry (RIPI), Tehran, Iran

Introduction

The most popular heteropoly acids are those having the Keggin structure, $H_3PW_{12}O_{40}$ (HPW). The main disadvantages of HPWs are high solubility in water and their very low surface area (less than 10 $m^2\ g^{-1}$), which hinders accessibility to the acidic sites. In addition, the HPW has excessive acidity and an overhigh cracking activity, which increases the probability to undergo secondary reactions [1–4]. By substituting a fraction of the proton with monovalent ions such as Cs^+, K^+, Rb^+ and Ag^+, the heteropoly acids are turned into insoluble salts, which can be used as a reasonably good heterogeneous solid acid catalyst. The Cs-exchanged Keggin-type heteropoly acid is also well maintained at high temperatures, usually over 500 °C [5–9]. There are many studies about the effect of Cs content in HPW on the catalytic performance of these catalysts in various catalytic processes [8, 10]. $H_3PW_{12}O_{40}$ and $Cs_xH_{3-x}PW_{12}O_{40}$ compounds have been used as catalysts in hydrocracking of extra-heavy oils and reported the optimum Cs content (x = 2.2) which induces the best activity in this process [5]. For overcoming the low surface area of HPW, a feasible way is to prepare supported HPW catalysts. One approach to obtain supported HPW catalysts is the impregnation of a support with a heteropoly acid solution followed by evaporation of the solvent. Several supports, such as silica–alumina [11], silica gel [12], silica [13] and BEA zeolite [14] have been used to enhance the dispersion of the HPW. In this case, the accessibility to HPW acid sites has been increased, while its solubility in polar media decreased [15]. Extensive studies have been carried out over Cs salt of HPA supported on metal oxides for the hydrocracking reaction [4, 12, 16]. The effect of Cs content on the catalytic performance of the reduced Ni–$Cs_xH_{3-x}PW_{12}O_{40}/Al_2O_3$ catalysts for hydrocracking of *n*-decane in the presence of thiophene and pyridine has been reported. The highest catalytic activity for these catalysts belongs to Ni–$CsH_2P_{12}W_{40}/Al_2O_3$ catalyst [16]. In another work, the behavior of non-sulfided bimetallic Ni–Co–$H_3PW_{12}O_{40}/SiO_2$ catalysts has been reported. The results indicated the promotional effects of Co to hydrocracking activity of these catalysts [17]. Generally, hydrocracking supported catalysts are bifunctional, i.e. the acid sites which provide the cracking function and metal sites with a hydrogenation–dehydrogenation function [18]. Hence, active hydrocracking catalysts are composed of acidic supports such as SiO_2, Al_2O_3, ZrO_2, active carbon, modified zeolite etc., and active metals (e.g. Mo, W) with promoters (e.g. Ni, Co) [19–23].

Since molybdenum is an active phase in conventional catalysts, in this work, we have used both molybdenum and HPW for preparing new catalysts. Thus, the series of M/$Cs_{1.5}H_{1.5}PW/Al_2O_3$ (M = Ni or/and Mo) nanocatalysts by impregnation method have been prepared and the synthesized samples characterized with conventional techniques. The effect of molybdenum on the catalytic activity of the nanocatalysts in hydrocracking of *n*-decane has also been studied.

Experimental

In this work, we have prepared the $M/Cs_{1.5}H_{1.5}PW/Al_2O_3$ (M = Ni or/and Mo) nanocatalysts by impregnation and characterized the synthesized samples with conventional methods. The catalytic activity of the nanocatalysts in hydrocracking of *n*-decane has also been studied.

The samples were prepared via two steps with the impregnation method. First, the alumina support (Sasol Chemical Co., specific surface area 273 $m^2\ g^{-1}$, 40–70 mesh) was impregnated with a solution containing the desired quantities of $Ni(NO_3)_2$ (BDH, 98%), $(NH_4)_6Mo_7O_{24}{\cdot}4H_2O$ (Merck, 99%), and Cs_2CO_3 (Merck, 99.99%). Impregnated samples were dried overnight at 120 °C and then calcined at 400 °C for 3 h using a heating ramp of 2 °C min^{-1}. In the second step, the obtained samples were impregnated with a solution containing the desired quantities of $H_3PW_{12}O_{40}$ (Merck, 99%). The obtained products were finally dried overnight at 120 °C without calcination.

Powder X-ray diffraction (XRD) patterns were obtained on X' Pert Pro diffractometer equipment with a copper anode (Cu K_α monochromatized radiation source, λ = 1.54056 Å). The surface area (BET), pore volume and pore size of the catalysts were measured using N_2 at − 196 °C on an adsorption instrument (Quantasorb, Quantachrome). The morphologies and quantative analysis of the samples were determined by field emission scanning electron microscopy (FE-SEM) on TESCAN Mira3-XMU microscope equipped with energy dispersive X-ray spectroscopy (EDX). Temperature programmed desorption (TPD) and temperature programmed reduction (TPR) studies were performed using a semiautomatic micrometrics TPD/TPR 2900 apparatus to investigate the acid properties and reduction behavior of the catalysts, respectively.

The catalytic performance of the prepared catalyst was evaluated in a 300 ml batch type stainless steel autoclave reactor (452 HC reactor, Parr instrument). Schematic diagram of the experimental setup for hydrocracking of *n*-decane is shown in Fig. 1. The reaction test was carried out as follows: 20 g of *n*-decane (Merck, 99%) was charged into a reactor and 2 g of catalyst was added to the reactor. After the leak test of the reactor and purging with hydrogen (99.999%) for three times to remove air from the reactor, all the catalysts were reduced by a flow of H_2 at 200 °C for 1 h during stirring at 300 rpm. Then the reactor was pressurized to 3 MPa with hydrogen and the reactor was heated to achieve the reaction temperature (300 °C), which took 4 h. The pressure and temperature were recorded continuously during the reaction using a data logging instrument (4842 reactor controller, Parr instrument). When reaction time elapsed, the reactor was rapidly quenched to the ambient temperature. The reactants and products were analyzed by a gas chromatograph (VARIAN model CP-3800) equipped with capillary column (100 m) and FID detector. For comparison, an industrial hydrocracking catalyst (NiMo/ASA) was applied for hydrocracking of *n*-decane under the same condition. Conversion of the hydrocracking process was calculated by Eq. 1 and selectivity of the catalyst to the desired product was obtained by Eq. 2.

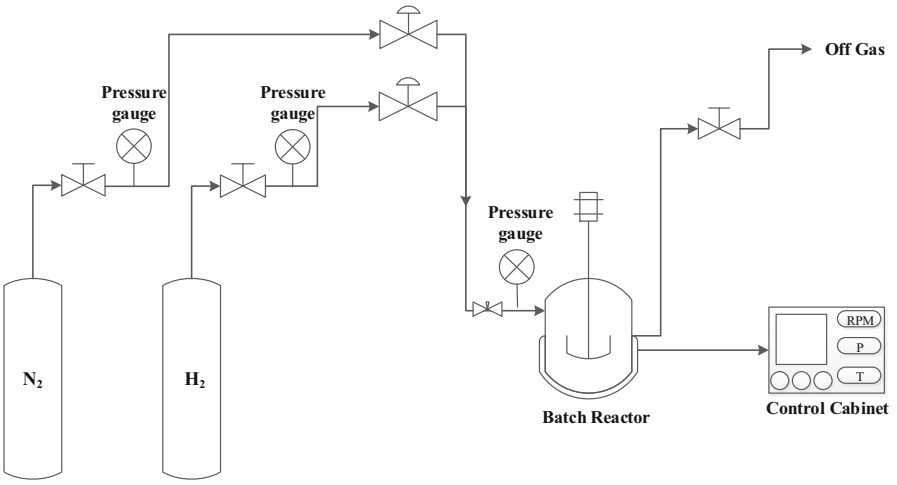

Fig. 1 Schematic diagram of the experimental setup for hydrocracking of *n*-decane in 300 ml batch type stainless steel autoclave reactor

$$Conversion\,\% = \frac{\sum X_i}{n_{Feed}} \times 100 \tag{1}$$

$$P_i\,Selectivity\,\% = \frac{X_i}{\sum X_i} \times 100 \tag{2}$$

here P_i is a desired product and X_i is mole number of P_i and n_{Feed} is mole number of the feed.

Results and discussion

The XRD patterns of the $M/Cs_{1.5}H_{1.5}PW/Al_2O_3$ (M = Ni or/and Mo) samples are presented in Fig. 2. The comparison of the XRD patterns of the prepared catalysts indicate that the keggin structure of $Cs_xH_{3-x}PW$ phase (10.5°, 18°, 23.6°, 25.9°, 30°, 35.1°, 54.3° and 62.2°) (JCPDS No:50-1857) is observed in the patterns [24, 25]. It is clear that no diffraction peaks of NiO (JCPDS No:73-1519), MoO_3 (JCPDS No:21-0569) and Al_2O_3 (JCPDS No:10-0425) appeared in the patterns. It is elucidated that Ni and Mo were dispersed well on the support and no segregation of those took place in impregnation process. The crystallite sizes of the prepared samples, calculated by the Scherrer equation using the intense peak (2θ = 26), are presented in Table 1. This table shows that the size of the prepared particles are in nanoscale.

Elemental analysis, surface area, pore volume and pore diameter of the samples are given in Table 1. The elemental composition of the prepared catalysts was examined via EDX. EDX analysis at different points on the samples also confirmed

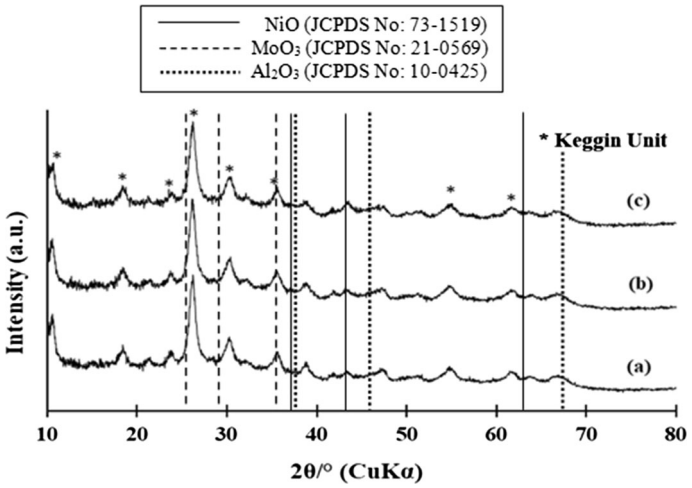

Fig. 2 XRD patterns of $M/Cs_{1.5}H_{1.5}PW/Al_2O_3$ (M = Ni or/and Mo) catalysts prepared by impregnation technique: **a** $Mo/Cs_{1.5}H_{1.5}PW/Al_2O_3$, **b** $Ni–Mo/Cs_{1.5}H_{1.5}PW/Al_2O_3$, **c** $Ni/Cs_{1.5}H_{1.5}PW/Al_2O_3$

Table 1 Elemental analysis results, crystallite size of the keggin structure of $Cs_xH_{3-x}PW$ phase (Calculated by Scherrer equation) and Physical properties of the catalysts

Catalyst	Element* (Wt%)					Surface area (m^2g^{-1})	Pore volume (cm^3g^{-1})	Pore size (nm)	Crystallite size (nm)
	Cs	Ni	Mo	P	W				
Al_2O_3	–	–	–	–	–	273	0.718	10.5	–
Mo/ $Cs_{1.5}H_{1.5}PW/$ Al_2O_3	4.6	–	3.70	0.79	37.6	126	0.271	8.6	10.23
Ni–Mo/ $Cs_{1.5}H_{1.5}PW/$ Al_2O_3	4.3	2.32	2.20	0.78	34.2	162	0.298	7.3	9.74
Ni/ $Cs_{1.5}H_{1.5}PW/$ Al_2O_3	4.5	4.20	–	0.68	35.8	156	0.305	7.9	9.98

*Calculated by EDX method

the uniform composition of the compound (Fig. 3). Table 1 also indicates that the surface area, pore volume and pore diameter of Al_2O_3 after impregnation decrease remarkably. It is reported that during impregnation the pore walls of Al_2O_3 can be eroded with acidic HPW aqueous solution and also the pores partially can be blocked with Ni/Mo species which lead to reducing the surface area of Al_2O_3 [12, 26, 27].

The FE-SEM images are indicated in Fig. 4. These images show that the synthesized particles are actually agglomerated and homogeneous nano-size crystallites are nearly in spherical shape.

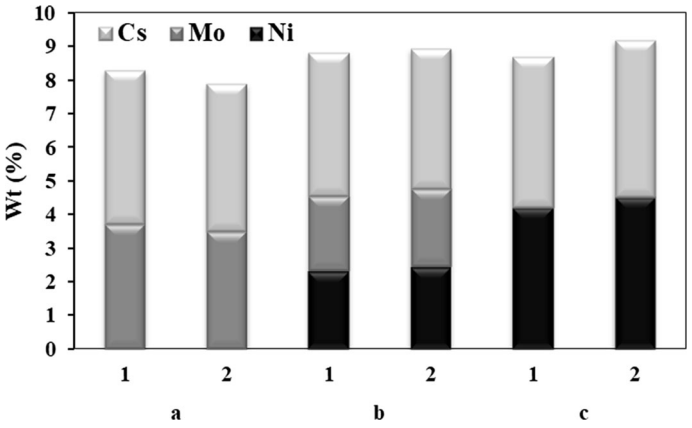

Fig. 3 Ni, Mo and Cs distribution observed at two points the samples by EDX for $M/Cs_{1.5}H_{1.5}PW/Al_2O_3$ (M = Ni or/and Mo) catalysts: **a** $Mo/Cs_{1.5}H_{1.5}PW/Al_2O_3$, **b** $Ni–Mo/Cs_{1.5}H_{1.5}PW/Al_2O_3$, **c** $Ni/Cs_{1.5}H_{1.5}PW/Al_2O_3$

To examine the acidic properties of the $M/Cs_{1.5}H_{1.5}PW/Al_2O_3$ (M = Ni or/and Mo) catalysts, NH_3–TPD was carried out. According to the experimental work of Jiang and et al. the strength of acidic sites can be classified by NH_3-desorption temperature as weak (150–350 °C), moderate (350–500 °C) and strong (≥ 500 °C) acidic sites [28]. The NH_3–TPD profiles of the prepared samples are shown in Fig. 5. All profiles presented an intense peak which can be assigned to weak acidic sites. In addition, these profiles indicate that moderate and strong acidic sites exist in the samples. These results show that in $Ni–Mo/Cs_{1.5}H_{1.5}PW/Al_2O_3$ catalyst weak and moderate acidic sites are more than the other catalysts, while strong acidic site in $Ni/Cs_{1.5}H_{1.5}PW/Al_2O_3$ catalyst is more than the other ones. These results also confirm that total acid sites of $Ni–Mo/Cs_{1.5}H_{1.5}PW/Al_2O_3$ catalyst is more than the others (Table 2). Increasing total acid sites can be correlated to the formation of $MoNiO_x$ phase. This result is in agreement with the literature [29]. Meng et al. reported that in NiMo/Beta-KIT-6 catalysts, all NiMo based catalysts contained both weak and moderate acid sites in NiMo/BK catalysts.

The H_2–TPR profiles of catalysts are shown in Fig. 6. It is interesting to notice that the reduction peak of NiO Bulk is not observed in these profiles. According to literature the NiO reduction peak appears at 300 °C [28]. Also, in the presence of H_3PW species, NiO reduction occurs at higher temperature around 530 °C [16]. When Cs replaces with H in H_3PW species, the interaction of NiO with these species is weaker and reduction occurs at lower temperature, so that the peaks observed at about 420–500 °C can be attributed to the reduction of Ni(II). The peak observed at about 490 °C for TPR profile of a sample could be assigned to reduction of Mo(VI) to Mo(IV) [30, 31]. This peak is also seen in Fig. 6b, which is covered by NiO reduction peak. The peaks at 680 °C and 710 °C can be attributed to different intermediate composition such as $Al_2(MoO_4)_3$ (Fig. 6a) [32]. These peaks can also be seen in Fig. 6b containing Ni and Mo, although they are overlap with a strong peak in the 700 °C. This strong peak corresponds to the reduction of Ni(II) that

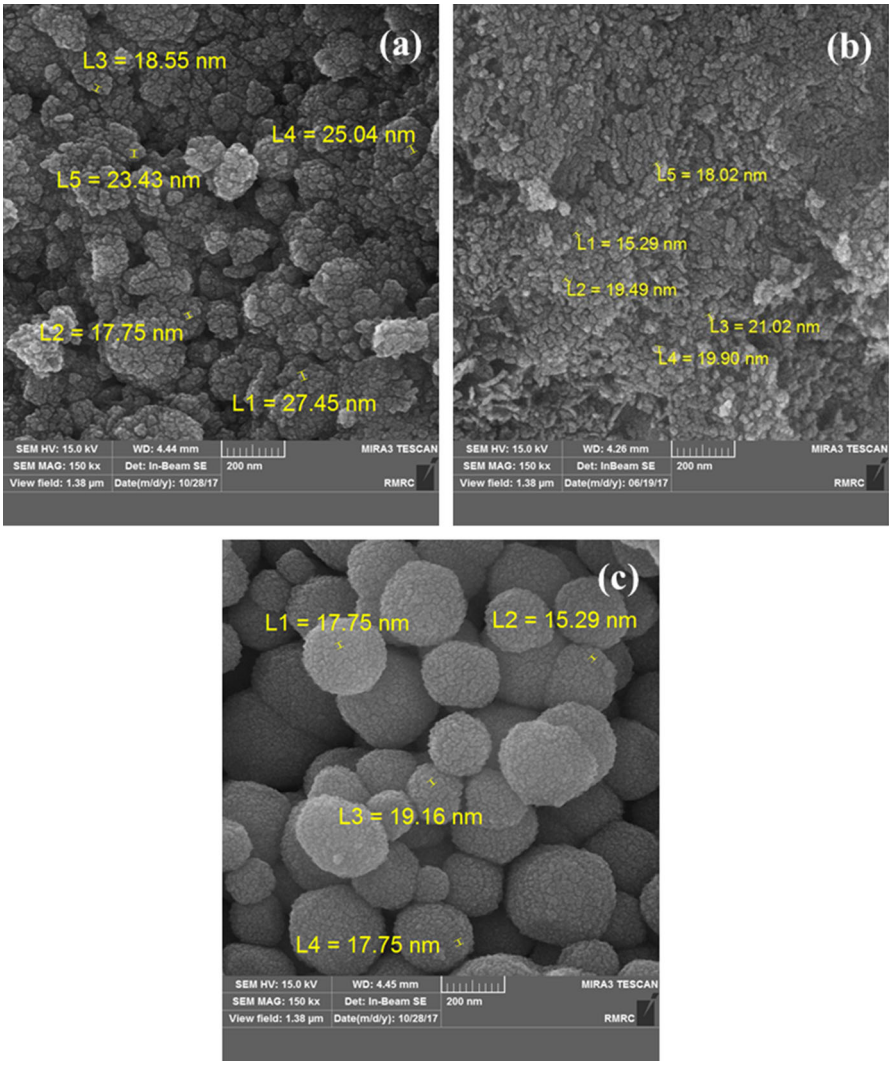

Fig. 4 FE-SEM images of catalysts prepared by impregnation technique: **a** $Mo/Cs_{1.5}H_{1.5}PW/Al_2O_3$, **b** $Ni–Mo/Cs_{1.5}H_{1.5}PW/Al_2O_3$, **c** $Ni/Cs_{1.5}H_{1.5}PW/Al_2O_3$

interacts with the support [33]. The reduction peak near 740 °C corresponds to the reduction of $Cs_{1.5}H_{1.5}PW$ species [14, 16]. It can be noticed from Table 2 that the H_2 consumption per gram of catalyst in $Ni–Mo/Cs_{1.5}H_{1.5}PW/Al_2O_3$ catalyst is higher than that of for the other samples that indicate higher reducibility of catalyst. It seems that the higher amount of H_2 consumption for $Ni–Mo/Cs_{1.5}H_{1.5}PW/Al_2O_3$ catalyst was related to $MoNiO_x$ phase which could be formed due to the reaction between Mo and Ni.

The catalytic evaluation results for the reduced $M/Cs_{1.5}H_{1.5}PW/Al_2O_3$ (M = Ni or/and Mo) catalysts in hydrocracking of *n*-decane are shown in Figs. 7 and 8 and

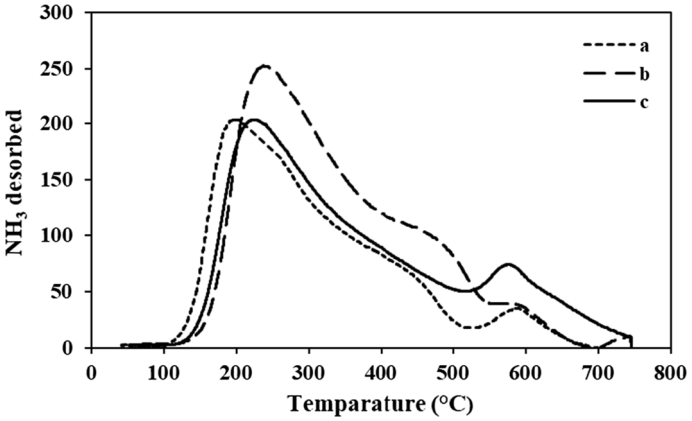

Fig. 5 NH3–TPD profiles of $M/Cs_{1.5}H_{1.5}PW/Al_2O_3$ (M = Ni or/and Mo) catalysts: **a** $Mo/Cs_{1.5}H_{1.5}PW/Al_2O_3$, **b** $Ni–Mo/Cs_{1.5}H_{1.5}PW/Al_2O_3$, **c** $Ni/Cs_{1.5}H_{1.5}PW/Al_2O_3$

Table 2 H_2 and NH_3 consumption (mmol/g) of the prepared nanocatalysts

Samples	H_2 consumption (mmol of H_2/g cat)	NH_3 consumption (mmol of NH_3/g cat) (total acidity)
$Mo/Cs_{1.5}H_{1.5}PW/Al_2O_3$	1.9456	0.6699
$Ni–Mo/Cs_{1.5}H_{1.5}PW/Al_2O_3$	3.9023	1.1295
$Ni/Cs_{1.5}H_{1.5}PW/Al_2O_3$	3.0890	1.0125

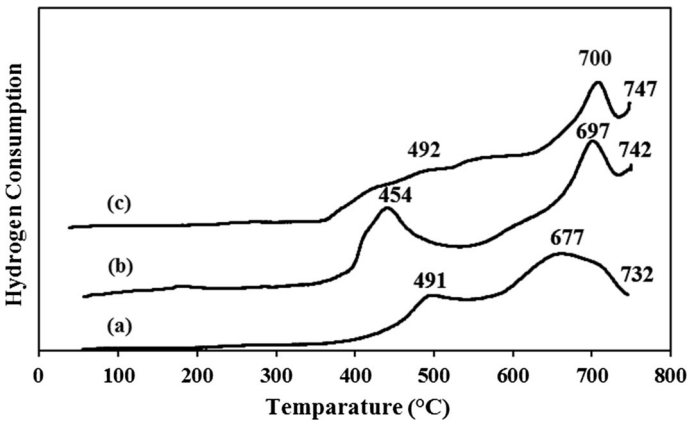

Fig. 6 H_2–TPR profiles of $M/Cs_{1.5}H_{1.5}PW/Al_2O_3$ (M = Ni or/and Mo) catalysts: **a** $Mo/Cs_{1.5}H_{1.5}PW/Al_2O_3$, **b** $Ni–Mo/Cs_{1.5}H_{1.5}PW/Al_2O_3$, **c** $Ni/Cs_{1.5}H_{1.5}PW/Al_2O_3$

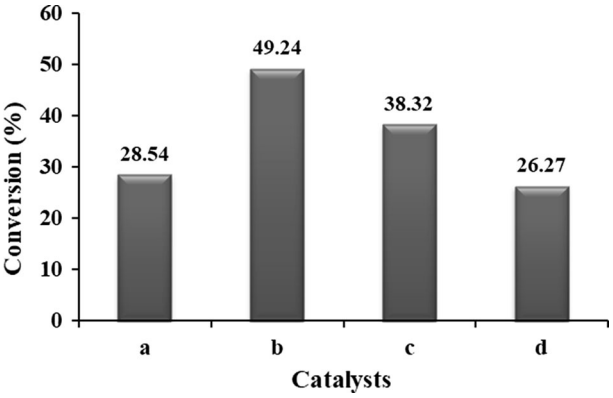

Fig. 7 Conversion of $M/Cs_{1.5}H_{1.5}PW/Al_2O_3$ (M = Ni or/and Mo) catalysts in hydrocracking of *n*-decane: (Reaction conditions: T = 300 °C, P = 3 MPa, t = 4 h, 20 g of *n*-decane and 2 g of the catalyst): **a** $Mo/Cs_{1.5}H_{1.5}PW/Al_2O_3$, **b** $Ni–Mo/Cs_{1.5}H_{1.5}PW/Al_2O_3$, **c** $Ni/Cs_{1.5}H_{1.5}PW/Al_2O_3$, **d** industrial catalyst

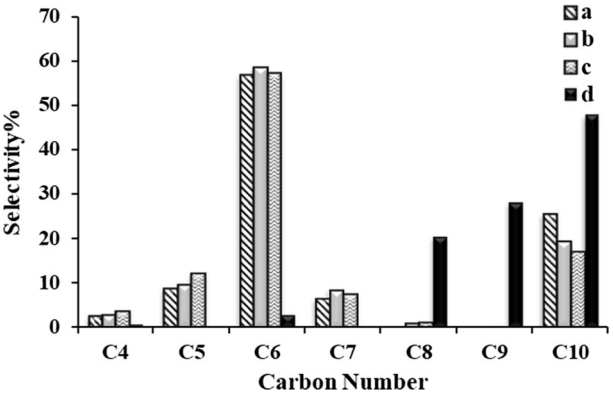

Fig. 8 Selectivity of $M/Cs_{1.5}H_{1.5}PW/Al_2O_3$ (M = Ni or/and Mo) catalysts in hydrocracking of *n*-decane: (Reaction conditions: T = 300 °C, P = 3 MPa, t = 4 h, 20 g of n-decane and 2 g of the catalyst): **a** $Mo/Cs_{1.5}H_{1.5}PW/Al_2O_3$, **b** $Ni–Mo/Cs_{1.5}H_{1.5}PW/Al_2O_3$, **c** $Ni/Cs_{1.5}H_{1.5}PW/Al_2O_3$, **d** industrial catalyst

Table 3 Selectivity of prepared nanocatalysts in hydrocracking of n-decane

Samples	Selectivity (%)						
	C_4	C_5	C_6	C_7	C_8	C_9	C_{10}
$Mo/Cs_{1.5}H_{1.5}PW/Al_2O_3$	2.6	8.8	56.7	6.4	0	0	25.5
$Ni-Mo/Cs_{1.5}H_{1.5}PW/Al_2O_3$	2.8	9.7	58.6	8.6	0.9	0	19.4
$Ni/Cs_{1.5}H_{1.5}PW/Al_2O_3$	3.8	12.2	57.3	7.6	1.2	0.5	17.4
Industrial catalyst	0.7	0	2.8	0	20.5	28.2	47.8

Table 3. The catalytic performance of the prepared catalysts was compared with that of a typical NiMo/ASA industrial catalyst. By addition of Ni to the Mo/$Cs_{1.5}H_{1.5}PW/Al_2O_3$ catalyst, the conversion of *n*-decane increases. Classically, the middle acidity amount of a catalyst would favor the hydrocracking activity [14]. In the Ni–Mo/$Cs_{1.5}H_{1.5}PW/Al_2O_3$ catalyst, weak and moderate acidic sites are more than the other catalysts and amount of total conversion of this catalyst is more than the others.

As can be observed in Fig. 7, the hydrocracking activity of Mo/$Cs_{1.5}H_{1.5}PW/Al_2O_3$ catalyst is low. By partially and completed substitution of Ni for Mo in the Mo/$Cs_{1.5}H_{1.5}PW/Al_2O_3$ catalyst, the order of catalysts activity is: Ni–Mo/$Cs_{1.5}H_{1.5}PW/Al_2O_3$ > Ni/$Cs_{1.5}H_{1.5}PW/Al_2O_3$ > Mo/$Cs_{1.5}H_{1.5}PW/Al_2O_3$. Meanwhile, the activities of the prepared catalysts are more than activity of industrial catalyst. Furthermore, the order of the acidity of the catalysts is coincident with the order of catalytic activity. It can be concluded that higher acidity leads to higher catalytic activity. It is evident that the activity of the Mo/$Cs_{1.5}H_{1.5}PW/Al_2O_3$ catalyst with addition of Ni increased from 28.54% to 49.24% while, the activity of Ni/$Cs_{1.5}H_{1.5}PW/Al_2O_3$ catalyst is lower than that of Ni–Mo/$Cs_{1.5}H_{1.5}PW/Al_2O_3$ catalyst. This result could be due to interaction between Ni and Mo, which leads to increasing the reducibility of Ni in this catalyst. This result is also proved by TPR experiment. Similar results were reported by B. Qiu and et al. for enhancing the reducibility of Ni–H_3PW/SiO_2 catalyst by Co, which increases the hydrocracking activity of such bimetallic catalyst [17].

The distribution of the obtained products in the presence of the prepared catalysts for hydrocracking of *n*-decane is shown in Fig. 8. For all the prepared catalysts the main products is C_6 hydrocarbons while the commercial catalyst leads to production of heavier hydrocarbon such as C_{10} hydrocarbons including 3-methyl C_9, 2-3-dimethyl C_8 and 3-3-4 trimethyl C_7. For all samples the amounts of $< C_4$ hydrocarbons are negligible and selectivity of the catalysts for these compounds are not considered in Fig. 8.

The production of C_{10} hydrocarbons in the presence of all the catalysts indicates that isomerization process is also occurred. However, this process is more notable for industrial catalyst. In addition, 94% of the C_6 components are branched hydrocarbons which confirm the isomerization process. Also, according to the results, it can be explained that the Ni–Mo/$Cs_{1.5}H_{1.5}PW/Al_2O_3$ catalyst has higher selectivity to C_6 products than the other catalysts. Thus, it is more likely that this catalyst produce middle distillate hydrocarbons in hydrocracking process. The use of the commercial catalyst resulted in a comparatively lower C_6 product selectivity (2.8%) compared to that of Ni–Mo/$Cs_{1.5}H_{1.5}PW/Al_2O_3$ catalyst (58.6%). In fact, all of the prepared catalysts were more proper than the commercial catalyst for producing the middle distillate products (see Table 3). Generally, the hydrocracking process usually carried out using a metal/acid bifunctional catalyst [14], over which the alkanes are dehydrogenated-hydrogenated on the metallic sites and hydrocracked on the acidic sites. The hydrocracking of *n*-decane on the M/$Cs_{1.5}H_{1.5}PW/Al_2O_3$ (M = Ni or/and Mo) catalysts occurs through bifunctional mechanism as well, hydrocracking mechanism on the acidic sites and hydrogenation reaction mechanism on the metallic sites. According to the aforementioned discussion, the

high activity of Ni–Mo/$Cs_{1.5}H_{1.5}PW/Al_2O_3$ catalyst for hydrocracking was apparently attribute to the unique structure of the HPW, which did not mere act as an acid site, but also cooperated with the hydrogenation metal site to act as hydrogen supply.

Conclusions

M/$Cs_{1.5}H_{1.5}PW/Al_2O_3$ (M = Ni or/and Mo) catalysts were successfully prepared by impregnation method and evaluated as catalyst for hydrocracking of *n*-decane. The obtained results indicated that using both molybdenum and nickel in these catalysts has an important role in chemical and physical properties and catalytic behavior of them in *n*-decane hydrocracking. The NH_3-TPD results indicate that in Ni–Mo/$Cs_{1.5}H_{1.5}PW/Al_2O_3$ catalyst weak and moderate acidic sites are more than the other catalysts, the catalyst shows the highest activity. The best result was obtained on the Ni–Mo/$Cs_{1.5}H_{1.5}PW/Al_2O_3$ catalyst with the C_6 selectivity of 58.5% and *n*-decane conversion of 49.24%. The results show that C_6 and C_{10} component are branched hydrocarbons which confirm the isomerization process is also occurred during hydrocracking process. Moreover, the interaction between the metal (Ni or/and Mo) and the $Cs_{1.5}H_{1.5}PW$ of the catalyst offers the sufficient reactive hydrogen on the surface of the catalysts.

References

1. Dai Y, Li BD, Quan HD, Lu CX (2010) $[Hmim]_3PW_{12}O_{40}$: a high-efficient and green catalyst for the acetalization of carbonyl compounds. Chin Chem Lett 21:678–681
2. Sheng JY, Qiu B, Jin H, Yi XD, Fang WP (2010) Alumina supported $H_3PW_{12}O_{40}$ and Ni catalysts for hydrocracking of *n*-decane. Asian J Chem 22:4439–4449
3. Bhure MH, Kumar I, Natu AD, Chikate RC, Rode CV (2008) Phosphotungstic acid on silica with modified acid sites as a solid catalyst for selective cleavage of tert-butyldimethylsilyl ethers. Catal Commun 9:1863–1868
4. Qiu B, Yi XD, Lin L, Fang WP, Wan HL (2008) The hydrocracking of *n*-decane over bifunctional Ni-$H_3PW_{12}O_{40}/SiO_2$ catalysts. Catal Today 131:464–471
5. Eom HJ, Lee D-W, Kim S, Chung S-H, Hur YG, Lee KY (2014) Hydrocracking of extra-heavy oil using Cs-exchanged phosphotungstic acid ($Cs_xH_{3-x}PW_{12}O_{40}$, x = 1–3) catalysts. Fuel 126:263–270
6. Misono M (2013) Catalysis of heteropoly compounds (polyoxometalates). In: Makoto M (ed) Studies in surface science and catalysis. Elsevier, New York, pp 97–155
7. Zeng ZX, Cui L, Xue WL, Ma KN (2013) Study on adsorption behavior of 12-phosphotungstic acid on silica gel. Ind Eng Chem Res 52:8070–8078
8. Shin H-Y, An S-H, Sheikh R, Park YH, Bae S-Y (2012) Transesterification of used vegetable oils with a Cs-doped heteropolyacid catalyst in supercritical methanol. Fuel 96:572–578
9. Geboers J, Van de Vyver S, Carpentier K, Jacobs P, Sels B (2011) Hydrolytic hydrogenation of cellulose with hydrotreated caesium salts of heteropoly acids and Ru/C. Green Chem 13:2167–2174
10. Parida KM, Rana S, Mallick S, Rath D (2010) Cesium salts of heteropoly acid immobilized mesoporous silica: an efficient catalyst for acylation of anisole. J Colloid Interface Sci 350:132–139
11. De Mattos FCG, De Carvalho ENCB, Freitas EFD, Paiva MF, Ghesti GF, Macedo JLD, Dias SC, Dias JA (2017) Acidity and characterization of 12-tungstophosphoric acid supported on silica-alumina. J Braz Chem Soc 28:336–347
12. Jin H, Yi X, Sun X, Qiu B, Fang W, Weng W, Wan H (2010) Influence of $H_4SiW_{12}O_{40}$ loading on hydrocracking activity of non-sulfide Ni–$H_4SiW_{12}O_{40}/SiO_2$ catalysts. Fuel 89:1953–1960

13. Jovic A, Bajuk-Bogdanovi D, Vasiljevi BN, Milojevi –Raki M, Krajisnik D, Dondur V, Popa A, Uskokovi-Markovi S, Holclajtner-Antunovi I (2017) Synthesis and characterization of 12-phosphotungstic acid supported on BEA zeolite. Mater Chem Phys 186:430–437
14. Jin H, Guo D, Sun X, Sun S, Liu J, Zhu H, Yang G, Yi X, Fang W (2013) Direct synthesis, characterization and catalytic performance of non-sulfided Ni–$CsxH_{3-x}PW_{12}O_{40}/SiO_2$ catalysts for hydrocracking of *n*-decane. Fuel 112:134–139
15. Haber J, Pamin K, Matachowski L, Mucha D (2003) Catalytic performance of the dodecatungstophosphoric acid on different supports. Appl Catal A 256:141–152
16. Jin H, Yi X, Sun S, Liu J, Yang G, Zhu H, Fan W (2012) Hydrocracking of n-decane over non-sulfided Ni-$Cs_xH_{3-x}PW_{12}O_{40}/Al_2O_3$ catalysts. Fuel Process Technol 97:52–59
17. Qiu B, Yi X, Li Lin, Fang W, Wan H (2009) Influence of the incorporation of cobalt on non-sulfided Ni–$H_3PW_{12}O_{40}/SiO_2$ hydrocracking catalysts. Catal Commun 10:1296–1299
18. Thybaut JW, Laxmi Narasimhan CS, Denayer JF, Baron GV, Jacobs PA, Martens JA (2005) Acid-metal balance of a hydrocracking catalyst: ideal versus nonideal behavior. Ind Eng Chem Res 44:5159–5169
19. Cui Q, Zhou Y, Wei Q, Yu G, Zhu L (2013) Performance of Zr- and P-modified USY-based catalyst in hydrocracking of vacuum gas oil. Fuel Process Technol 106:439–446
20. Looi PY, Mohamed AR, Tye CT (2012) Hydrocracking of residual oil using molybdenum supported over mesoporous alumina as a catalyst. Chem Eng J 181–182:717–724
21. Tiwari R, Rana BS, Kumar R, Verma D, Kumar R, Joshi RK (2011) Hydrotreating and hydrocracking catalysts for processing of waste soya-oil and refinery-oil mixtures. Catal Commun 12:559–562
22. Leyva C, Rana MS, Trejo F, Ancheyta J (2009) NiMo supported acidic catalysts for heavy oil hydroprocessing. Catal Today 141:168–175
23. Leyva C, Rana MS, Trejo F (2007) On the use of acid-base-supported catalysts for hydroprocessing of heavy petroleum. Ind Eng Chem Res 46:7448–7466
24. Corma A, Martinez A, Martinez C (1996) Acidic Cs^+, NH_4^+, and K^+ salts of 12-tungstophosphoric acid as solid catalysts for isobutane/2-butene alkylation. J Catal 164:422–432
25. Narasimharao K, Brown DR, Lee AF, Newman AD, Siril PF, Avener SJ (2007) Structure–activity relations in Cs-doped heteropolyacid catalysts for biodiesel production. J Catal 248:226–234
26. Ameen M, Azizan MT, Ramli A, Yusup S, Yasir M (2016) Physicochemical properties of Ni-Mo/γ-Al_2O_3 catalysts synthesized via sonochemical method. Procedia Eng 148:64–71
27. Liu HP, Lu GZ, Guo Y, Wang YQ, Guo YL (2009) Synthesis of mesoporous Pt/Al_2O_3 catalysts with high catalytic performance for hydrogenation of acetophenone. Catal Commun 10:1324–1329
28. Jiang J, Dong Z, Chen H, Sun J, Yang Ch, Cao F (2013) The Effect of additional zeolites in amorphous silica–alumina supports on hydrocracking of semirefined paraffinic wax. Energy Fuels 27:1035–1042
29. Meng J, Wang Z, Ma Y, Lu J (2017) Hydrocracking of low-temperature coal tar over NiMo/Beta-KIT-6 catalyst to produce gasoline oil. Fuel Process Technol 165:62–71
30. Solı´s D, Agudo AL, Ramı´rez J, Klimova T (2006) Hydrodesulfurization of hindered dibenzothiophenes on bifunctional NiMo catalysts supported on zeolite–alumina composites. Catal Today 116:469–477
31. Qu L, Zhang W, Kooyman PJ, Prins R (2003) MAS NMR, TPR, and TEM studies of the interaction of NiMo with alumina and silica–alumina supports. J Catal 215:7–13
32. Brito J, Laine J (1986) Characterization of supported MoO_3 by temperature programmed reduction. Polyhedron 5:179–182
33. Marzari JA, Rajagopal S, Miranda R (1995) Bifunctional mechanism of pyridine hydrodinitrogenation. J Catal 156:255–264